Computational and Theoretical Chemistry 1212 (2022) 113723

Contents lists available at ScienceDirect

Computational and Theoretical Chemistry

journal homepage: www.elsevier.com/locate/comptc

Reactive molecular dynamics and DFT simulations of FTDO explosive

Rene F.B. Gonçalves [a], Aleksey Kuznetsov [b,*], Bruno T. Rocco [c], Leopoldo Rocco Jr. [c], José A.F. F. Rocco [a]

[a] Departamento de Química - Instituto Tecnológico de Aeronáutica - CTA, São José dos Campos/SP, Brasil
[b] Department of Chemistry, Universidad Técnica Federico Santa Maria, Av. Santa Maria 6400, Vitacura, Santiago, Chile
[c] Flowtest Engenharia e Pesquisa Ltda., Caieiras/SP, Brasil

ARTICLE INFO

Keywords:
Furazanotetrazinedioxide
Pyrolysis
Reactive molecular dynamics
DFT
Activation energy

ABSTRACT

This paper presents the results of the Density Functional Theory (DFT) calculations and reactive molecular dynamics (RMD) simulations of the furazanotetrazinedioxide (FTDO) explosive, a novel highly energetic material. The details of the mechanism of the FTDO decomposition have been elucidated for the first time. The calculated activation energy was found to be 30.96 ± 2.25 kJ/mol. The DFT calculation results suggested that FTDO is prone to the fragmentation and decomposition processes. The study results present original mechanisms for the FTDO detonation/decomposition along with the values for the activation energy and frequency factor with high linear determination coefficient.

1. Introduction

Energetic materials have been broadly used in both civil and military areas; compounds such as nitroglycerin, black powder, and nitrocellulose have been among the most used over the last few decades [1–11]. Among the characteristic properties of these compounds and/or formulations, the ability to release a large amount of energy in a short period of time when exposed to thermal or electrical stimulation or due to an impact can be highlighted. Due to these characteristics, numerous studies have been performed with the focus on increasing the performance of these energetic materials [1–10]. Explosives usually contain nitrogen, oxygen and/or other oxidizers in their composition, so the combustion process can occur extremely fast and without the need for an external oxidizer [2,12]. The most common explosives currently used are TNT, RDX, and HMX [13], however, CL-20, PETN, and TATP are also potent and perspective energetic materials, despite of their handling difficulties. Research of novel explosives is being constantly developed, and 1,2,5-oxadiazolo[3,4-*e*]-1,2,3,4-tetrazine-4,6-dioxide or furazanotetrazine dioxide (FTDO) is one of the most recent explosives under investigation (Fig. 1). FTDO is one of the most powerful explosives ever known [14,15]. Its synthesis was first reported in 1995 [16] and later several alternative synthetic methods were reported not involving nitronium salts [17–20]. Despite the noticeably high sensitivity of the pristine FTDO to mechanical stresses [21], this compound is quite attractive as a component of various high-energy compositions due to its high formation enthalpy, ΔH_f^0, varying within 158–176.5 kcal mol^{-1} [22–24], and relatively high density, d^{20}, 1.84–1.85 g cm^{-3} [19,25]. The detonation rate of an FTDO single crystal was found to be as high as 9.14 km/s [15].

Due to its outstanding properties, FTDO has been the subject of several computational investigations and its applications are currently being analyzed and tested. However, it should be emphasized that the computational studies of FTDO are relatively scarce so far. Thus, in 2007, the standard enthalpy of formation of FTDO was calculated using a theoretical value of its formation heat in the gas phase and an experimentally measured value of its sublimation enthalpy [22]. The calculations were performed using the G2, G3, and CBS-QB3 high-accuracy multilevel quantum chemical approaches. In 2019, Baraboshkin *et al.* reported the combined X-ray study and computational modeling of the FTDO-benzene (1:1) solvated structure [15]. Using the atom–atom potentials method, the original methodology and elaborated program packages, the crystal structure of the pure FTDO was predicted. Optimizations of molecular structures were performed using the restricted Hartree-Fock method with the 6-31G(d,p) basis. In 2014, Lai *et al.* reported the structural investigation of FTDO using density functional theory (DFT) method (B3LYP functional with cc-pvdz and 6-31G** basis sets) [26]. The FTDO stability was evaluated by potential energy surface scanning and structure interconversion thermodynamics under different temperatures. The spontaneous isomerization of FTDO and its effects on the FTDO stability were investigated as well. The dissociation of FTDO

* Corresponding author.
E-mail address: aleksey.kuznetsov@usm.cl (A. Kuznetsov).

https://doi.org/10.1016/j.comptc.2022.113723
Received 23 February 2022; Received in revised form 5 April 2022; Accepted 20 April 2022
Available online 30 April 2022

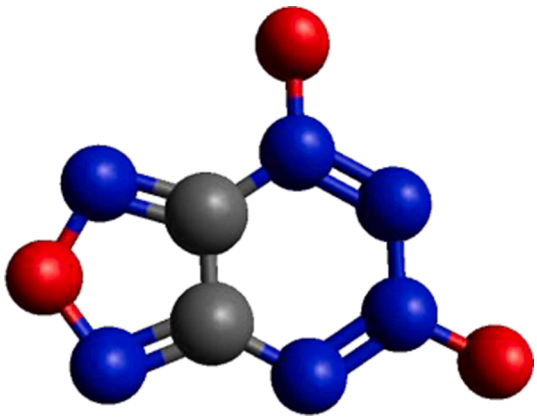

Fig. 1. FTDO structure.

to N_2, N_2O, and furoxan fragments was also studied. Recently, Zelenov *et al.* reported a quantum chemical simulation of the cocrystal structures of FTDO with benzotrifuroxan (BTF) in ratios of 1:1, 2:1, and 3:1, along with the results of the studies of their thermodynamic stability and physical–chemical characteristics [27]. According to their calculations, the (3:1) cocrystal was found to be thermodynamically the most stable structure. An *ab initio* simulation of the crystal structures of FTDO–BTF cocrystals was carried out in the framework of the atom–atom potentials method. The geometry and distribution of the molecular electrostatic potential (MEP) of the BTF and FTDO molecules were obtained by B3PW91 calculations with the 6-31G(d,p) basis set.

Combustion and explosive behavior of energetic materials are experimentally difficult to analyze, so the chemical mechanisms and the elementary steps of these processes for FTDO are not well-known so far. The combination of quantum mechanical calculations with the reactive molecular dynamics (RMD) methodologies enables *ab initio* analyses of various materials, thus providing the most probable structures and behavior during combustion or pyrolysis along with means to determine the mechanism and kinetics of the whole process.

Reactive molecular dynamics has been proved useful for simulating energetic materials in several studies of physical–chemical characterization [28,29], catalyst analysis [30,31] or combustion/detonation performance analysis [32,33]. HMX and RDX, two of the most common and effective explosives, were studied by molecular dynamics methods. Zhu *et al.* (2009) [34] analyzed the structure of pure RDX and RDX bonded with different polymers (PBX), thus gaining better understanding of their mechanical properties, binding energies, and detonation performances. The force fields used in RMD simulations are built using quantum mechanical methodologies, therefore there are many groups developing different force fields for studying combinations or formulations of energetic materials [35]. Zhang *et al.* in 2009 [36] and Wu *et al.* in 2020 [37] studied the thermal decomposition of HMX under different conditions, showing that RMD methods are reliable and can be used to assist in the development of new materials or technologies.

In the current study we present the results of the FTDO investigation using DFT and RMD simulations aimed at evaluation of its structure, electronic properties, mechanism of pyrolysis, and stability. The kinetic parameters of the FTDO pyrolysis were determined based on an Arrhenius model approach. The mechanisms for the pyrolysis process were elucidated, based on the behavior of the participating species during the decomposition.

The paper is organized as follows. In the next section, we provide first the details of DFT methodology and next the details of RMD simulations. Then, the results of the RMD simulations of pyrolysis and DFT studies of the structural, electronic, and reactivity features are provided and discussed. Finally, conclusions and perspectives of future research are given.

2. Methodology

2.1. DFT studies

DFT studies of FTDO were performed employing the Gaussian 09 software, revision B.01 [38]. We optimized the FTDO geometry in the singlet state and C_s symmetry and then performed frequency calculations to ensure that the optimized structure indeed is the energy minimum. The calculations were done using the hybrid density functional B3LYP [39] along with the split-valence polarized basis set 6-311+G* [40,41], having a set of diffuse functions and a set of polarization functions, in the gas phase (vacuum). This approach is furthermore referred to as B3LYP/6-311+G*. The analysis of charge distribution was performed using the Natural Bond Orbital (NBO) method as implemented in the Gaussian 09 software [42,43], using the B3LYP/6-311+G* approach. Frontier molecular orbitals (FMOs) were calculated at the B3LYP/6-311+G* level. Below we consider calculated structural parameters, NBO charges, and frontier molecular orbitals of the B3LYP/6-311+G* optimized structure. Furthermore, we used the values of the energies of the HOMO (highest occupied molecular orbital) and LUMO (lowest unoccupied molecular orbital) and the values of the HOMO/LUMO gaps to calculate the values of global reactivity parameters (GRP) [44,45] (Eqs. (1)–(6) below). Eqs. (1) and (2) were used to calculate the values of the ionization potential (*IP*) and electron affinity (*EA*):

$$IP = -E_{\mathrm{HOMO}} \tag{1}$$

$$EA = -E_{\mathrm{LUMO}} \tag{2}$$

For global hardness η and electronegativity X values we used Eqs. (3) and (4):

$$\eta = \frac{[IP - EA]}{2} = \frac{[E_{LUMO} - E_{HOMO}]}{2} \tag{3}$$

$$X = \frac{[IP - EA]}{2} = \frac{[E_{LUMO} + E_{HOMO}]}{2} \tag{4}$$

And global electrophilicity ω value was calculated by Eq. (5):

$$\omega = \frac{\mu^2}{2\eta} \tag{5}$$

where $\mu = \frac{[E_{HOMO}+E_{LUMO}]}{2}$ is the chemical potential of the system.

Finally, the global softness σ value was computed with the Eq. (6):

$$\sigma = \frac{1}{2\eta} \tag{6}$$

Open GL version of Molden 5.8.2 visualization program was used for the visualization of the structure and FMOs of the title compound [46], and Avogadro, version 1.1.1, was used to visualize the molecular electrostatic potential (MEP) [47,48].

2.2. Reactive molecular dynamics simulations

Molecular-scale pyrolysis reactions of FTDO was simulated using LAMMPS (Large-scale Atomic/Molecular Massively Parallel Simulator) software [49,50], which has high applicability for molecular dynamics (MD) studies of solid-state materials (metals, semiconductors) and soft matter (biomolecules, polymers), as well as coarse-grained or mesoscopic systems. It can be used to model atoms or, more generically, as a parallel particle simulator at the atomic, meso, or continuum scale.

The resolution of MD equations through the ReaxFF model [51] of interatomic interactions provides a complete description of the temporal evolution of the system, which includes the formation and breaking of chemical bonds. In this force field, the general energy function takes the following formulation:

$$E_{system} = E_{bond} + E_{over} + E_{under} + E_{val} + E_{pen} + E_{tors} + E_{conj} + E_{vdWaals} + E_{Coulomb} \quad (7)$$

where

- E_{bond} represents the bond energy;
- E_{over} and E_{under} denotes the over- and under-coordinated atom in the energy contribution, respectively;
- E_{val}, E_{pen}, E_{tors} are the valence angle term, penalty energy and torsion energy, respectively;
- E_{conj}, $E_{vdWaals}$ and $E_{Coulomb}$ represent the conjugation effects to molecular energy, nonbonding van der Waals interactions and Coulomb interactions, respectively.

MD simulation results also enable kinetic analysis of the chemical reactions by allowing to calculate the reaction Arrhenius parameters. Kinetic parameters are calculated based on the reactant consumption with the time course. Using the first-order approach, the rate constant is calculated for each temperature applied in the system. Then, the linearized Arrhenius equation is applied to obtain the activation energy (E_a) and the frequency factor (A) values.

The pyrolysis simulation was performed using the condensed phase structure of FTDO, at eleven different temperatures ranging from 1000 to 2000 K. In a unit cell with the dimensions 13.26 × 23.72 × 26.12 Å 59 molecules of FTDO were placed, generating a condensed phase structure with approximate density of 1.86 g cm^{-3} (experimental density: 1.86 g cm^{-3} [52]). For the simulations, the domain size was increased to 58.00 × 68.00 × 71.00 Å, thus allowing free expansion of the molecules, as periodic boundary conditions were applied in three dimensions. The domain expansion was done to prevent interactions among the boundaries. During the temperature increase, the system may expand, thus reducing the overall density. Low-temperature energy minimization was performed with 100 maximum amounts of iterations and the system was then equilibrated at 200 K employing the canonical ensemble, using a linear temperature increase from 5 to 200 K during 10 ps, then it was maintained at constant temperature. Different equilibration times were used for the simulations, varying from 20 to 45 ps, so the results presented are averaged over all simulations. For the production phase the NVT was also applied during 100 ps, with the temperatures in the range of 1000 to 2000 K, controlled by a Nose-Hoover thermostat with damping frequency of 100 steps.

3. Results and discussion

Pyrolysis simulations of energetic materials have been of utmost importance. Depending on the conditions, these materials may detonate or deflagrate. Thus, their behavior when subjected to increasing temperatures can reveal some of their most important properties. In this work, FTDO was subjected to the isothermal simulations, with the temperatures ranging from 1000 K to 2000 K. Fig. 2 presents a comparison of the first decomposition process development over time depending on the decomposition temperature. As expected, the increase of temperatures leads to faster decomposition of the substance.

In RMD simulations, the temperature is supplied to the system in terms of velocity, i.e., spatial displacements of the atoms. High temperatures are used to speed up the process and to reduce the computational costs of the simulations. As the timestep used was 0.1 fs, a high number of interactions is needed to evaluate the behavior of the system in a minimum amount of time (in this case, the simulation time was 100 ps). Therefore, high temperatures are applied to the system for enabling reactions (bonds breakage/formation) in the timeframe selected.

As previously stated, one of the simulation results is the variation of the species number over time. As the species decompose, new ones are produced, which may participate in other reactions, thus following a specific reaction mechanism. Each elementary reaction/step observed can occur both forward and backward, having specific activation energies, reaction enthalpies etc. Therefore, the mechanism is totally dependent on the system temperature.

Table 1 presents the elementary reactions with the highest occurrences during the FTDO pyrolysis over 100 ps for each simulation temperature. Only forward reactions are presented, as our aim is to show the difference in occurrences at different temperatures. As observed, different temperatures lead to different mechanisms, with various number of reaction occurrences, as every elementary step has specific kinetic/thermodynamic parameters. Higher temperatures lead to the increase of the collision frequency, so the probability of chemical reactions increases substantially. Also, reactions with higher energetic barriers (activation energies) become feasible when the atoms/

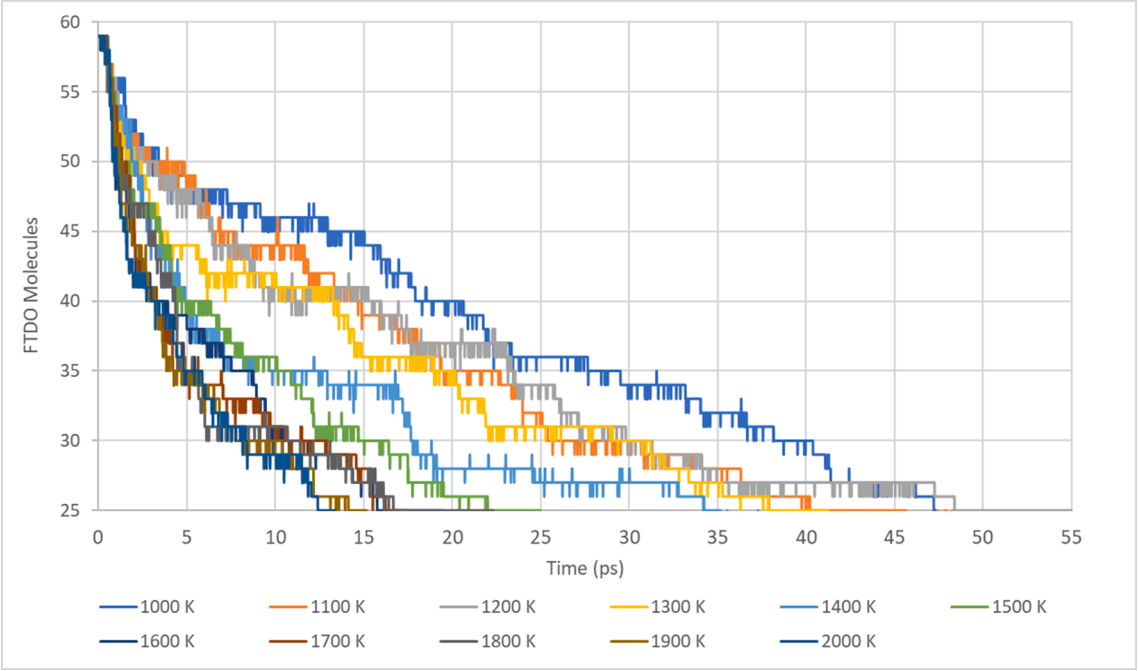

Fig. 2. FTDO molecules decomposition over time in different isothermal simulations.

Table 1
Most occurring elementary reactions (forward) for the FTDO decomposition for each set temperature.

Reaction	Occurrence										
	1000 K	1100 K	1200 K	1300 K	1400 K	1500 K	1600 K	1700 K	1800 K	1900 K	2000 K
1 C2N6O3 <> 1O + 1 C2N6O2	81	66	72	34	37	35	17	17	20	11	17
1 C2N6O3 <> 1 C2N5O3 + 1 N	94	73	113	76	34	48	17	26	31	18	24
1 C2N6O3 <> 1 NO + 1 C2N5O2	15	7	89	9	8	5	5	6	2	5	3
1 C2N6O3 <> 1 C2N4O2 + 1 N2O	12	17	4	4	6	6	6	3	6	1	12
1 C2N5O3 <> 1 NO + 1 C2N4O2	130	72	1	89	1	0	1	202	59	116	0
1 C2N5O3 <> 1 CNO + 1 CN4O2	14	22	0	15	0	0	0	19	17	14	0
1 C2N4O2 <> 1 NO + 1 C2N3O	17	36	19	21	17	20	10	41	16	12	10
1 C2N4O2 <> 1 C2N2O + 1 N2O	23	34	30	13	28	17	24	19	11	29	25
1 C2N3O <> 1 NO + 1 C2N2	78	17	42	54	8	38	36	29	14	7	31
1 C2N3O <> 1 N2 + 1 C2NO	26	0	0	1	0	0	0	1	2	2	0
1 C2N2 + 1O <> 1 C2N2O	31	54	88	33	53	73	61	46	29	47	25
1 N2O <> 1 N2 + 1O	1	2	4	0	583	71	10	132	696	117	21
1 C2NO <> 1 CN + 1 CO	0	1	1	52	0	0	46	20	80	24	119
1 NO + 1O <> 1 NO2	2	5	1	0	0	16	1	6	47	14	42

molecules have increased velocities due to the temperature variation. The first two reactions (initiation steps) are preferable over the others for lower temperatures. There are several initiation reactions, but only the main reactions were presented; in the systems with higher temperatures the initiation reaction occurrence is more equilibrated, as there is enough energy for any of the reactions to be activated.

Initiation steps where FTDO molecules lose an atom and radicals (intermediate species) are produced and participate in the propagation reactions are easily observed. Like most of the mechanisms, the propagation steps are the most numerous ones, with formation and decomposition of numerous radicals and other species. As the number of radicals and other species decreases, the termination steps start leading the process, thus producing the main pyrolysis products (in this specific case, CN, CO, NO, and NO_2). Faster product formation is observed at higher temperatures, due to the consequent increase in the reaction rates.

Application of the Arrhenius rate law over the FTDO concentration range enabled the calculations of the FTDO pyrolysis kinetic parameters (Fig. 3), with their values provided in Table 2. The E_a value calculated for the system is noticeably lower than the literature reported value [10,11], which might be explained by the peculiarities of the reaction force field optimization. Energetic materials are hazardous substances, and FTDO is one of the materials with higher detonation potential, when compared to the other common explosives like HMX, RDX, CL-20 or PETN [29]. Therefore, it is not uncommon to observe a low activation energy for this material. Experimental determination of these properties, if possible, is troublesome, especially for reactive and sensitive substances.

3.1. DFT study results

In Fig. 4 the optimized FTDO structure along with the FMOs and MEP

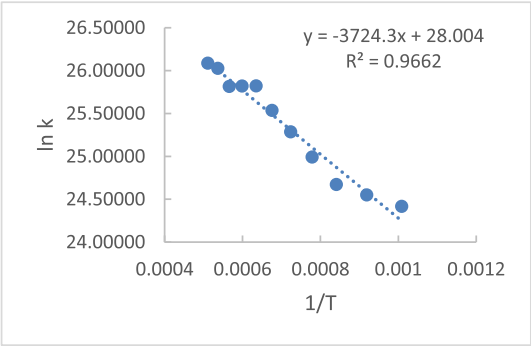

Fig. 3. Arrhenius fit for the FTDO decomposition.

Table 2
Calculated kinetic parameters for the FTDO pyrolysis.

	E_a (kJ/mol)	A (1/s)
Calculated	30.96 ± 2.25	1.45 ± 0.11E + 12
Experimental [10,11]	110.77	–

plots are provided. As can be seen from Fig. 4a, two N—O bonds attached to the six-membered ring are not equal, being different by 0.013 Å, and all N—N bonds in this ring are also noticeably unequal, varying within 1.307–1.464 Å. In the azole ring two N—O bonds are also unequal, being different by 0.024 Å. Also, these bonds are noticeably longer than the N—O bond distances in the six-membered ring, by ca. 0.15–0.16 Å. The C—N bond distances in both rings are noticeably unequal as well. Furthermore, the valence angle N4-N1-O1 is noticeably smaller than 120°. In general, the molecule should be considered as a quite strained species. It should be noticed that the results of our calculations are in nice agreement with the results provided by Lai *et al.* [26].

Results of natural charges calculation, as shown in Table 3, demonstrate that all three oxygens of FTDO bear quite high negative charges, −0.117 to −0.307e, with the higher negative charges on the terminal oxygens O1 and O2. Among the nitrogens, the highest negative charge, −0.252e, is accumulated on N3, whereas the atoms N1 and N2, bound with terminal oxygens, bear significant positive charges, 0.407e and 0.285e, respectively. Interestingly, the N's in the oxazole ring bear relatively low negative charges, especially N6. The two carbons of the molecule have high positive charges. Again, these results are in nice agreement with the results obtained by Baraboshkin *et al.* [15] and Zelenov *et al.* [27], even though the schemes for charge calculations used are different.

The HOMO and LUMO of FTDO both are of a" symmetry and have contributions from both rings (Fig. 4b). HOMO is essentially dominated by contributions from the azole ring and from the N1-O1 group, whereas LUMO is dominated by contributions from non-carbon atoms of the molecule. It can be seen that HOMO provides bonding interactions between two rings of the molecule and within the rings, whereas LUMO essentially provides antibonding interactions within the oxazole and six-membered rings. The MEP plot (Fig. 4c) shows accumulation of positive electrostatic potential on the bridging carbons (as indicated by blue color) and certain accumulations of negative electrostatic potential on three oxygens, as indicated by reddish color.

The consideration of the calculated global reactivity parameters, provided in Table 4, shows the following. (i) The FTDO molecule has high ionization potential value, 8.72 eV, along with quite high electron affinity value, 4.96 eV. This implies that FTDO would not lose electrons

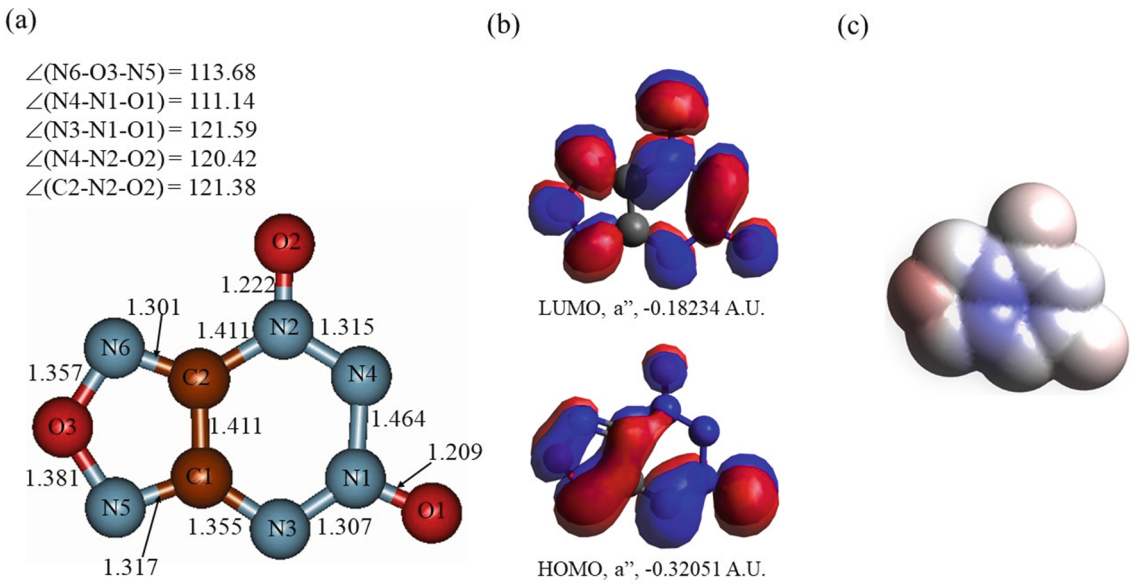

Fig. 4. The optimized structure (a), HOMO and LUMO plots (b), and MEP plot (c) of FTDO. Color mapping: brown for C, blue for N, red for O. Bond distances are given in Å, bond angles are given in degrees. (For interpretation of the references to color in this figure legend, the reader is referred to the web version of this article.)

Table 3
Natural charges, e, on the FTDO atoms (numbering scheme according to Fig. 4a).

Atom	N1	N2	N3	N4	N5	N6	O1	O2	O3	C1	C2
Charge, e	0.407	0.285	−0.252	−0.106	−0.059	−0.009	−0.296	−0.307	−0.117	0.245	0.209

Table 4
The FTDO calculated GRPs (eV).

E_{HOMO}	E_{LUMO}	$\Delta E_{(HOMO/LUMO)}$	ΔE_{TDDFT}	IP	EA	X	η	μ	σ	ω
−8.72	−4.96	3.76	3.29	8.72	4.96	6.84	1.88	−6.84	0.266	12.44

due to oxidation but rather would readily attain electrons, which would lead to bond breakage in its molecule and its further decomposition. (ii) Next, the values of global electronegativity X as well as global electrophilicity ω for FTDO, 6.84 and 12.44 eV, respectively, should be considered as noticeably high (especially the ω value), which implies that this compound would act as a strong oxidizer/electron acceptor, which is also supported by its high EA value. (iii) The FTDO global hardness value, η, 1.88 eV, is noticeably small, and its global softness σ value, 0.266, is quite low, too.

These results imply that FTDO should be considered as a quite reactive compound, which would behave in redox reactions as a noticeably strong electron acceptor or oxidizer. Furthermore, attachment of electrons to the LUMO of the FTDO molecule would cause extra repulsions and increase antibonding interactions withing the azole and six-membered rings, which, in turn, would result in bond breaking and decomposition of the molecule, thus making it quite unstable towards reduction.

Also, it is interesting to notice that no experimentally measured HOMO/LUMO gap values or TDDFT gap values calculated by other researchers can be found. Therefore, due to the fact that TD-B3LYP is considered as underestimating the TDDFT gaps for some systems [53], we decided to make control calculations of this gap using the TDDFT with the ωB97XD [54] and BLYP [55,56] functionals. The first functional, which uses a version of Grimme's D2 dispersion model, gave noticeably larger gap value compared to TD-B3LYP (3.29 eV), 3.84 eV, whereas the second functional, the combination of the Becke exchange functional (B) and the LYP correlation functional, gave noticeably lower gap value compared to TD-B3LYP, 2.84 eV. The TD-DFT calculation with the ωB97XD functional gave the gap values relatively close to the B3LYP calculated HOMO/LUMO gap value, 3.76 eV (see Table 4).

4. Conclusions and perspectives

Here we have reported the first combination of the comprehensive DFT study (structure, natural charge distribution, FMOs, MEP, and reactivity parameters) and detailed analysis of the FTDO decomposition behavior by RMD calculations, using eleven different temperatures in isothermal simulations. The mechanism for the FTDO decomposition has been elucidated in detail showing significant differences among the occurrences of each elementary reaction, therefore proving that, when a small increase on the system temperature occurs, different elementary steps are activated and become feasible in each situation. Kinetic parameters were calculated for the overall process, using the Arrhenius approach for the set of simulations.

The DFT results showed that FTDO should be considered as quite strained molecule, highly prone to electron attachment and thus significantly prone to fragmentation and decomposition processes. The charges in the FTDO molecule were studied using more sophisticated NBO approach, and the global reactivity parameters for the compound in the gas phase have been first time determined, implying the FTDO increased reactivity.

Thus, the first combined DFT and RMD study of the important highly energetic compound, FTDO, has been reported. The results obtained will definitely fill the gaps in the knowledge about this species and assist in

further studies and design of high-energy *N*-containing compounds.

The following questions might be the subject of the follow-up studies.

(1) Detailed study of thermodynamics (reaction enthalpies and activation barriers, intermediate structures) of the most important processes of the FTDO pyrolysis, partially based on the results of Lai *et al.* [26].
(2) Detailed studies of the FTDO properties in various solvents: possible effects on the structure, explicit solvation with different small molecules, solvent effects on charges and reactivity parameters.
(3) Detailed investigation of various co-crystals of FTDO, as stimulated by the works of Baraboshkin *et al.* [15] and Zelenov *et al.* [27]: types and energies of intermolecular interactions, charge distribution, electronic properties, etc.

CRediT authorship contribution statement

Rene F.B. Gonçalves: Funding acquisition, Supervision, Project administration, Conceptualization, Methodology, Data curation, Visualization, Investigation, Formal analysis, Validation, Writing – original draft, Writing – review & editing, Resources. **Aleksey Kuznetsov:** Project administration, Conceptualization, Methodology, Data curation, Visualization, Investigation, Formal analysis, Validation, Writing – original draft, Writing – review & editing. **Bruno T. Rocco:** Methodology, Data curation, Visualization, Investigation, Formal analysis, Validation, Writing – original draft, Writing – review & editing, Resources. **Leopoldo Rocco:** Methodology, Data curation, Visualization, Investigation, Formal analysis, Validation, Writing – original draft, Writing – review & editing, Resources. **José A.F.F. Rocco:** Funding acquisition, Supervision, Project administration, Conceptualization, Methodology, Data curation, Visualization, Investigation, Formal analysis, Validation, Writing – original draft, Writing – review & editing, Resources.

Declaration of Competing Interest

The authors declare that they have no known competing financial interests or personal relationships that could have appeared to influence the work reported in this paper.

Acknowledgements

The authors would like to thank the Brazilian agency CNPq (National Council for Scientific and Technological Development) for financial support, project Universal 2018, process 406726/2018-3. Aleksey Kuznetsov acknowledges the computational resources of supercomputer cluster in Instituto Tecnológico de Aeronáutica (ITA), Brazil.

References

[1] J.J. Sabatini, L.A. Wingard, P.E. Guzman, E.C. Johnson, G.W. Drake, Bis-Isoxazole dinitrate: A potential propellant and explosive ingredient. 42nd International Pyrotechnics Society Seminar, Grand Junction, 2016.
[2] J.C. Oxley, The Chemistry of Explosives, in: J.A. Zukas, W.P. Walters (Eds.), Explosive Effects and Applications, 1st ed., Springer Science, New York, 2003, pp. 137–172.
[3] P.R. Lee, Explosives development and fundamentals of explosives technology, in: J. A. Zukas, W.P. Walters (Eds.), Explosive Effects and Applications, 1st ed., Springer Science, New York, 2003, pp. 23–46.
[4] W.C.L. Silva, Blast - efeitos da onda de choque no ser humano e nas estruturas, Tese de Mestrado, Instituto Tecnológico de Aeronáutica, Brasil, 2007.
[5] V. Dharma Rao, A. Srinivas Kumar, K. Venkateswara Rao, V.S.R. Krishna Prasad, Theoretical and Experimental Studies on Blast Wave Propagation in Air, Propellants, Explos., Pyrotech. 40 (2015) 138.
[6] G. da Silva, N.M. Nakamura, K. Iha, Kinetic study of the thermal decomposition of pentaerythritol-tetranitrate (PETN), Quim. Nova 31 (2008) 2060.
[7] E. Kirchhof, R.J. Rocha, N.M. Nakamura, C.M. Lapa, G.F.M. Pinheiro, R.F. B. Gonçalves, J.A.F.F. Rocco, K. Iha, Estimate of PbX (Plastic-Bonded Explosive) Shelf Life with Accelerated Aging, Quim. Nova 39 (2016) 661.
[8] R.J. Rocha, J.E.S. Lima, S.R. Gomes, K. Iha, J.A.F.F. Rocco, Synthesis of modified polyurethanes based on castor oil employed in energetic materials, Quim. Nova 36 (2013) 793.
[9] G. Silva, C. Mattos, M. Nakamura, K. Iha, Aplicação da Calorimetria Exploratoria Diferencial no Estudo da Cinetica de Transicao α → δ HMX, Quim. Nova 27 (2004) 889.
[10] V.P. Sinditskii, A.V. Burzhava, V.Y.A.B. Egorshev, A.B. Sheremetev, V.P. Zelenov, Combustion of furazanotetrazine dioxide, Combust Explos. Shock Waves 49 (2013) 117–120, https://doi.org/10.1134/S0010508213010139.
[11] V. Pepekin, Yu. Matyushin, T. Gubina, Enthalpy of formation and explosive properties of 5,6-(3,4-furazano)-1,2,3,4-tetrazine-1,3-dioxide. Russ. J. Phys, Chem. B. 2011, 5, 97-100. doi:10.1134/ S1990793111020102.
[12] H.-H. Zong, C. Yao, C.Q. Sun, J.-G. Zhang, L. Zhang, Structure and Stability of Aromatic Nitrogen Heterocycles Used in the Field of Energetic Materials. Molecules 2020, 25, 3232. doi:10.3390/ molecules25143232.
[13] S. Chatterjee, U. Deb, S. Datta, C. Walther, D.K. Gupta, Common explosives (TNT, RDX, HMX) and their fate in the environment: Emphasizing bioremediation, Chemosphere 184 (2017) 438–451, https://doi.org/10.1016/j.chemosphere.2017.06.008. Epub 2017 Jun 4 PMID: 28618276.
[14] R.F.B. Goncalves, B.T. Rocco, L. Rocco Jr., J.A.F.F. Rocco, Reactive Molecular Dynamics Simulation of FTDO Explosive, J. Phys.: Conf. Series 1507 (2020) 082046.
[15] N.M. Baraboshkin, V.P. Zelenov, A.V. Dzyabchenko, I.V. Fedyanin, T.S. Pivina, X-ray study and computational model of the solid solvate of [1,2,5]oxadiazolo[3,4-e][1,2,3,4]tetrazine 4,6-dioxide (FTDO) with benzene and ab initio crystal structure prediction of pure FTDO, J. Mol. Struct. 1190 (2019) 135–143.
[16] A.M. Churakov, S.L. Ioffe, V.A. Tartakovsky, Synthesis of [1,2,5]Oxadiazolo[3,4-e][1,2,3,4]tetrazine 4,6-Di-N-oxide, Mend. Commun. 6 (1995) 227–228, https://doi.org/ 10.1070/MC1995v005n06ABEH000539.
[17] A.M. Churakov, V.A. Tartakovsky, Progress in 1,2,3,4-tetrazine chemistry, Chem. Rev. 104 (2004) 2601–2616, https://doi.org/10.1021/CR020094Q.
[18] X. Li, B. Wang, H. Li, Y. Li, F. Bi, H. Huo, X. Fan, Novel synthetic route and characterization of [1,2,5] oxadiazolo [3,4-e][1,2,3,4]tetrazine 4,6-di-N-oxide (FTDO), Chin. J. Org. Chem. 32 (2012) 1975–1980, https://doi.org/10.6023/cjoc201205019.
[19] B. Wang, X. Li, H. Li, H. Huo, Y. Zhou, X. Fan, J. Li, A Novel Synthesis Route of [1,2,5]-Oxadiazolo[3,4-e][1,2,3,4]tetrazine-4,6-Di-N-oxide, Chin. J. Energetic Mater. 21 (2013) 131–132, https://doi.org/10.3969/j.issn.1006-9941.2013.01.027.
[20] V.P. Zelenov, A.A. Lobanova, S.V. Sysolyatin, N.V. Sevodina, New syntheses of [1,2,5]oxadiazolo[3,4-e][1,2,3,4]tetrazine 4,6-dioxide, Russ. J. Org. Chem. 49 (2013) 455–465, https://doi.org/10.1134/S107042801303024X.
[21] V.A. Teselkin, Mechanical sensitivity of furazano-1,2,3,4-tetrazine-1,3-dioxide, Combust. Explos. Shock Waves 45 (2009) 632–633, https://doi.org/10.1007/s10573-009-0076-7.
[22] V.G. Kiselev, N.P. Gritsan, V.E. Zarko, P.I. Kalmykov, V.A. Shandakov, Multilevel quantum chemical calculation of the enthalpy of formation of [1,2,5]oxadiazolo [3,4-e][1,2,3,4]-tetrazine-4,6-di-N-dioxide, Combust. Explos. Shock Waves 43 (2007) 562–566, https://doi.org/10.1007/s10573-007-0074-6.
[23] V.I. Pepekin, Tendencies in the development of studies of high explosives, Russ. J. Phys. Chem. B. 4 (2010) 954–962, https://doi.org/10.1134/S1990793110060138.
[24] K.R. Jorgensen, G.A. Oyedepo, A.K. Wilson, Highly energetic nitrogen species: Reliable energetics via the correlation consistent Composite Approach (ccCA). J. Hazard Mater. 186 (2011) 583–589, https://doi.org/ 10.1016/J.JHAZMAT.2010.11.035.
[25] A.S. Zharkov, P.I. Kalmykov, Y.N. Burtsev, N.P. Kuznetsova, I.A. Merzhanov, N. V. Chukanov, V.V. Zakharov, G.V. Romanenko, K.A. Sidorov, V.E. Zarko, Phase equilibria and structural phase transformations in the furazano[3,4-e]tetrazine-4,6-dioxidee2,4-dinitro-2,4-diazapentane system, Russ. Chem. Bull. 63 (2014) 1785–1800, https://doi.org/10.1007/s11172-014-0668-6.
[26] W.-P. Lai, P. Lian, T. Yu, J.-H. Bu, Y.-Z. Liu, W.-L. Zhu, J. Lv, Z.-H. Ge, Theoretical study on the structure and stability of [1,2,5]oxadiazolo [3,4-e] [1,2,3,4]-tetrazine-4,6-Di-N-dioxide (FTDO), J. Mol. Model. 20 (2014) 2343.
[27] V.P. Zelenov, N.M. Baraboshkin, D.V. Khakimov, N.V. Muravyev, D.B. Meerov, I. A. Troyan, T.S. Pivina, A.V. Dzyabchenko, I.V. Fedyanin, Time for quartet: the stable 3:1 cocrystal formulation of FTDO and BTF – a high-energy-density material, CrystEngComm 22 (2020) 4823.
[28] R.F.B. Goncalves, B.K.V. Iha, J.A.F.F. Rocco, A.E. Kuznetsov, Reactive molecular dynamics of pyrolysis and combustion of alternative jet fuels: A ReaxFF study, Fuel 310 (Part B) (2022) 122157.
[29] K. Yang, L. Chen, D.-Y. Liu, D.-S. Geng, J.-Y. Lu, J.-Y. Wu, Liu D-y, Geng D-s, Lu J-y, Wu J-y, Quantitative prediction and ranking of the shock sensitivity of explosives via reactive molecular dynamics simulations, Defence Technol. (2022).
[30] Sunday Temitope Oyinbo, Tien-Chien Jen, Hydrogen evolution reaction in an alkaline environment through nanoscale Ni, Pt, NiO, Fe/Ni and Pt/Ni surfaces: Reactive molecular dynamics simulation, Mater. Chem. Phys. 271, 2021, 124886.
[31] Sunday Temitope Oyinbo, Tien-Chien Jen, Reactive molecular dynamics simulations of nickel-based heterometallic catalysts for hydrogen evolution in an alkaline KOH solution, Computat. Mater. Sci. 201, 2022, 110860.
[32] B.W. Hamilton, B.A. Steele, M.N. Sakano, M.P. Kroonblawd, I.-F.-W. Kuo, A. Strachan, Predicted Reaction Mechanisms, Product Speciation, Kinetics, and Detonation Properties of the Insensitive Explosive 2,6-Diamino-3,5-dinitropyrazine-1-oxide (LLM-105), J. Phys. Chem. A 125 (2021) 1766–1777.

[33] Y. Wang, G.u. Mingyan, W.u. Jiajia, L. Cao, Y. Lin, X. Huang, Formation of soot particles in methane and ethylene combustion: A reactive molecular dynamics study, Int. J. Hydrogen Energy 46 (73) (2021) 36557–36568.
[34] W. Zhu, J. Xiao, W. Zhu, H. Xiao, Molecular dynamics simulations of RDX and RDX-based plastic-bonded explosives, J. Hazar. Mater. 164 (2009) 1082–1088.
[35] W. Zhu, X. Wang, J. Xiao, W. Zhu, H. Sun, H. Xiao, Molecular dynamics simulations of AP/HMX composite with a modified force field, J. Hazar. Mater. 167 (2009) 810–816.
[36] L. Zhang, S.V. Zybin, A.C.T. van Duin, S. Dasgupta, W.A. Goddard III, E.M. Kober, Carbon Cluster Formation during Thermal Decomposition of Octahydro-1,3,5,7-tetranitro-1,3,5,7-tetrazocine and 1,3,5-Triamino-2,4,6-trinitrobenzene High Explosives from ReaxFF Reactive Molecular Dynamics Simulations, J. Phys. Chem. A 113 (2009) 10619–10640.
[37] J. Wu, L. Yang, Y. Li, M. Sultan, D. Geng, L. Chen, Microscopic Mechanisms of Femtosecond Laser Ablation of HMX from Reactive Molecular Dynamics Simulations, J. Phys. Chem. C 124 (2020) 11681–11693.
[38] M.J. Frisch, G.W. Trucks, H.B. Schlegel, G.E. Scuseria, M.A. Robb, J.R. Cheeseman, G. Scalmani, V. Barone, B. Mennucci, G.A. Petersson, H. Nakatsuji, M. Caricato, X. Li, H.P. Hratchian, A.F. Izmaylov, J. Bloino, G. Zheng, J.L. Sonnenberg, M. Hada, M. Ehara, K. Toyota, R. Fukuda, J. Hasegawa, M. Ishida, T. Nakajima, Y. Honda, O. Kitao, H. Nakai, T. Vreven, J.A. Montgomery Jr., J.E. Peralta, F. Ogliaro, M. Bearpark, J.J. Heyd, E. Brothers, K.N. Kudin, V.N. Staroverov, R. Kobayashi, J. Normand, K. Raghavachari, A. Rendell, J.C. Burant, S.S. Iyengar, J. Tomasi, M. Cossi, N. Rega, J.M. Millam, M. Klene, J.E. Knox, J.B. Cross, V. Bakken, C. Adamo, J. Jaramillo, R. Gomperts, R.E. Stratmann, O. Yazyev, A.J. Austin, R. Cammi, C. Pomelli, J.W. Ochterski, R.L. Martin, K. Morokuma, V.G. Zakrzewski, G.A. Voth, P. Salvador, J.J. Dannenberg, S. Dapprich, A.D. Daniels, Ö. Farkas, J. B. Foresman, J.V. Ortiz, J. Cioslowski, D.J. Fox, Gaussian 09, Revision B.01, Gaussian, Inc., Wallingford CT, 2009.
[39] A.D. Becke, Density-functional thermochemistry. III. The role of exact exchange, J. Chem. Phys. 98 (1993) 5648–5652.
[40] A.D. McLean, G.S. Chandler, Contracted Gaussian-basis sets for molecular calculations. 1. 2nd row atoms, Z=11-18, J. Chem. Phys. 72 (1980) 5639–5648.
[41] K. Raghavachari, J.S. Binkley, R. Seeger, J.A. Pople, Self-Consistent Molecular Orbital Methods. 20. Basis set for correlated wave-functions, J. Chem. Phys. 72 (1980) 650–654.
[42] A.E. Reed, R.B. Weinstock, F. Weinhold, Natural-population analysis, J. Chem. Phys. 83 (1985) 735–746.
[43] A.E. Reed, L.A. Curtiss, F. Weinhold, Intermolecular interactions from a natural bond orbital, donor-acceptor viewpoint, Chem. Rev. 88 (1988) 899–926.
[44] P.K. Chattaraj (Ed.), Chemical Reactivity Theory. A Density Functional View, CRC Press, 2020.
[45] P. Geerlings, F. De Proft, W. Langenaeker, Conceptual density functional theory, Chem. Rev. 103 (2003) 1793–1874.
[46] G. Schaftenaar, J.H.M. Noordik, a pre- and post-processing program for molecular and electronic structures, J. Comp.-Aided Mol. Des. 14 (2000) 123–134.
[47] Avogadro: an open-source molecular builder and visualization tool. Version 1.1.1. http://avogadro.cc/.
[48] M.D. Hanwell, D.E. Curtis, D.C. Lonie, T. Vandermeersch, E. Zurek, G.R. Hutchison, Avogadro: An advanced semantic chemical editor, visualization, and analysis platform, J. Cheminform. 4 (2012) 17.
[49] S. Plimpton, Fast Parallel Algorithms for Short-Range Molecular Dynamics, J. Comp. Phys. 117 (1995) 1–19.
[50] A.P. Thompson, H.M. Aktulga, R. Berger, D.S. Bolintineanu, W.M. Brown, P. S. Crozier, P.J. in 't Veld, A. Kohlmeyer, S.G. Moore, T.D. Nguyen, R. Shan, M. J. Stevens, J. Tranchida, C. Trott, S.J. Plimpton, a flexible simulation tool for particle-based materials modeling at the atomic, meso, and continuum, Comp. Phys. Commun. 271 (2022) 108171.
[51] A.C.T. van Duin, S. Dasgupta, F. Lorant, W.A. Goddard, ReaxFF: A reactive force field for hydrocarbons, J. Phys. Chem. A 105 (2001) 9396–9409.
[52] H.E. Ling, L.-L. Dong, G.-Q. Zhang, B.-S. Tan, M. Huang, G.-H. Tao, Structure and Properties of Furazano[3,4-e-1,2,3,4-tetrazine-1,3-dioxide, Chin. J. Energ. Mater. 20 (2012) 693–696.
[53] G. Zhang, C.B. Musgrave, Comparison of DFT Methods for Molecular Orbital Eigenvalue Calculations, J. Phys. Chem. A 111 (8) (2007) 1554–1561.
[54] J.-D. Chai, M. Head-Gordon, Systematic optimization of long-range corrected hybrid density functionals, J. Chem. Phys. 128 (2008), 084106.
[55] A.D. Becke, Density-functional exchange-energy approximation with correct asymptotic-behavior, Phys. Rev. A 38 (6) (1988) 3098–3100.
[56] C. Lee, W. Yang, R.G. Parr, Development of the Colle-Salvetti correlation-energy formula into a functional of the electron density, Phys. Rev. B 37 (1988) 785–789.